Geophysical Prospecting EAGE EUROPEAN ASSOCIATION OF GEOSCIENTISTS & ENGINEERS

Geophysical Prospecting, 2013, **61**, 42–52 doi: 10.1111/j.1365-2478.2012.01059.x

Dip-adaptive singular-value decomposition filtering for seismic reflection enhancement

Milton J. Porsani[1]*, Bjorn Ursin[2], Michelângelo G. Silva[3] and Paulo E. M. Melo[4]

[1]*Centro de Pesquisa em Geofísica e Geologia (CPPG/UFBA) and National Institute of Science and Technology of Petroleum Geophysics (INCT-GP/CNPQ). Instituto de Geociências, Universidade Federal da Bahia Campus Universitário da Federação, Salvador, Bahia, Brazil* [2]*The Norwegian University of Science and Technology, Department of Petroleum Engineering and Applied Geophysics. S.P. Andersensvei 15A, NO-7491 Trondheim, Norway* [3]*Centro de Pesquisa em Geofísica e Geologia (CPPG/UFBA) Instituto de Geociências, Universidade Federal da Bahia Campus Universitário da Federação, Salvador, Bahia, Brazil, and* [4]*Universidade Federal de Sergipe and National Institute of Science and Technology of Petroleum Geophysics (INCT-GP/CNPQ). Instituto de Geociências, Universidade Federal da Bahia Campus Universitário da Federação, Salvador, Bahia, Brazil.*

Received January 2011, revision accepted December 2011

ABSTRACT

We present a singular value decomposition (SVD) filtering method for the enhancement of coherent reflections and for attenuation of noise. The method is applied in two steps. First normal move-out (NMO) correction is applied to shot or CMP records, with the purpose of flattening the reflections. We use a spatial SVD filter with a short sliding window to enhance coherent horizontal events. Then the data are sorted in common-offset panels and the local dip is estimated for each panel. The next SVD filtering is performed on a small number of traces and a small number of time samples centred around the output sample position. Data in a local window are corrected for linear moveout corresponding to the dips before SVD. At the central time sample position, we sum over the dominant eigenimages of a few traces, corresponding to SVD dip filtering. We illustrate the method using land seismic data from the Tacutu basin, located in the north-east of Brazil. The results show that the proposed method is effective and is able to reveal reflections masked by ground-roll and other types of noise.

Key words: Local dip, Eigenimage, SVD filtering.

INTRODUCTION

Singular value decomposition (SVD) is a coherency-based technique that provides both signal enhancement and noise suppression. It has been implemented in a variety of seismic applications. Freire and Ulrych (1988) applied SVD filtering to the separation of upgoing and downgoing waves in vertical seismic profiling. Tyapkin, Marmalyevskyy and Gornyak (2003) proposed to use the data alignment method of Liu (1999) to make the coherent noise horizontally aligned in one or more time sections of a common shot gather. The noise is represented by the first eigenimages and the remaining eigenimages represent the signal. Chiu and Howell (2008) proposed a method that uses SVD to compute eigenimages that represent coherent noise in localized time-space windows. The data in the local windows are transformed into an analytic signal and followed by a complex SVD to decompose the analytic signal into eigenimages that represent the coherent noise model. Melo, Porsani and Silva (2009) presented a filtering method for ground-roll attenuation that uses a 2D time-derivative filter. Bekara and van der Baan (2007) proposed a local SVD approach to noise removal. In each data window the signal is horizontally aligned in time and after SVD only the first eigenimage is retained. Then the procedure is repeated in the next data window using sliding windows with a 50% overlap. Porsani et al. (2009, 2010a) used SVD filtering to attenuate ground-roll. Before the SVD computation, normal move-out (NMO) correction is applied to the seismograms, with the

*Email: porsani@cpgg.ufba.br

purpose of flattening the reflections. SVD is performed on a small number of traces in a sliding window filtering approach. The output trace is the central trace of the first few eigenimages. This technique was improved by Porsani et al. (2010b) by adding a second step of SVD filtering along the local dip on common-offset panels.

Here we further expand on this by proposing a seismic data processing scheme for noise attenuation in two steps. First we correct the seismic data for NMO so that the primary reflections are horizontally aligned along the x-axis. Then SVD filtering is applied in sliding windows on CMP or shot gathers (Porsani et al. 2009, 2010a). Since we are using a small spatial window, (3–5) traces, in the SVD and only keeping a few of the central eigentraces, amplitudes and frequency content are well preserved. Even NMO stretch will not be too much affected as the filter is applied locally.

In the second step we perform SVD filtering on common-offset panels. Now the local dip is estimated at all points in each offset panel and linear moveout is applied along the local dip in local space-time windows. Then dip-adaptive SVD filtering is applied in each window. This will enhance all dominant events in the sections. If there are crossing events, the weaker events may be degraded.

The proposed data processing strategy was successfully applied to a land seismic data set. Pre-stack common-shot and common-offset panels show a significant improvement in signal quality.

SPATIAL SINGULAR-VALUE DECOMPOSITION FILTERING

Following the procedure proposed by Porsani et al. (2009) we consider a seismic data set $d(t, x_n)$ where the time axis is given in the sample number, $t = 1, 2, \ldots, N_t$ and the space axis is given in the relative space position $x_n, n = 1, 2, \ldots, N_x$. The primary reflections were corrected for NMO so that they are horizontally aligned in the x-direction. A windowed data set of $2M + 1$ traces centred at x_n is given by a matrix with components $d(t, x_{n+j}), t = 1, \ldots, N_t, j = -M, \ldots, 0, \ldots, M$. It can be represented by the reduced SVD (Golub and van Loan, 1996):

$$d(t, x_{n+j}) = \sum_{k=1}^{2M+1} \sigma_k u_k(t) v_k(j). \tag{1}$$

Here the singular values are sorted such that $\sigma_1 \geq \sigma_2 \geq \cdots \geq \sigma_{2M+1} \geq 0$. In the filtered output data set only the first K eigenimages of the centre trace are being used. The output is

$$\tilde{d}(t, x_n) = \sum_{k=1}^{K} \sigma_k u_k(t) v_k(0). \tag{2}$$

The procedure is started at $n = M + 1$ where the filtered output is the sum of the K eigenimages corresponding to the K largest singular values of the first $M + 1$ traces:

$$\tilde{d}(t, x_{M+1+j}) = \sum_{k=1}^{K} \sigma_k u_k(t) v_k(j)\ , \quad j = -M, \ldots, 0. \tag{3}$$

Then n is increased by one and equation (2) is used until $n = N_x - M$ where the output data are given by the sum of the K first eigenimages of the last $M + 1$ traces. This is

$$\tilde{d}(t, x_{N_x-M+j}) = \sum_{k=1}^{K} \sigma_k u_k(t) v_k(j),\ j = 0, \ldots, M. \tag{4}$$

The sliding window scheme is shown in Fig. 1 for a window of 5 traces ($M = 2$). The result is a filtered data set $\tilde{d}(t, x_n)$ of the same dimension as the input data set where energy, which is not coherent in the x-direction, was attenuated. Both the character and amplitude of the horizontal events are well preserved as they are represented by the sum of centre trace of the first eigenimages that have the largest energy.

DIP-ADAPTIVE SPACE AND TIME SINGULAR-VALUE DECOMPOSITION FILTERING

This method is applied in the common-offset domain. For each data point $\{t, x_n\}$ the local dip is estimated using a total least squares approach (Van Huffel and Vandewalle 1991), as described in the Appendix. A linear moveout correction along the local dip is used to horizontally align the data in time-space windows.

The result is a windowed data set of $2L_x + 1$ traces and $2L_t + 1$ samples centred at $\{t, x_n\}$ given by a matrix with components

$$\hat{d}(t + i,\ x_{n+j}) \begin{cases} i = -L_t, \ldots, 0, \ldots, L_t, \\ j = -L_x, \ldots, 0, \ldots, L_x. \end{cases} \tag{5}$$

As in the previous case, the data matrix may be represented in terms of SVD

$$\hat{d}(t + i,\ x_{n+j}) = \sum_{k=1}^{2L_x+1} \sigma_k u_k(i) v_k(j). \tag{6}$$

To preserve the most significant amplitudes along the reflectors we use only the first K SVD components of the centre of

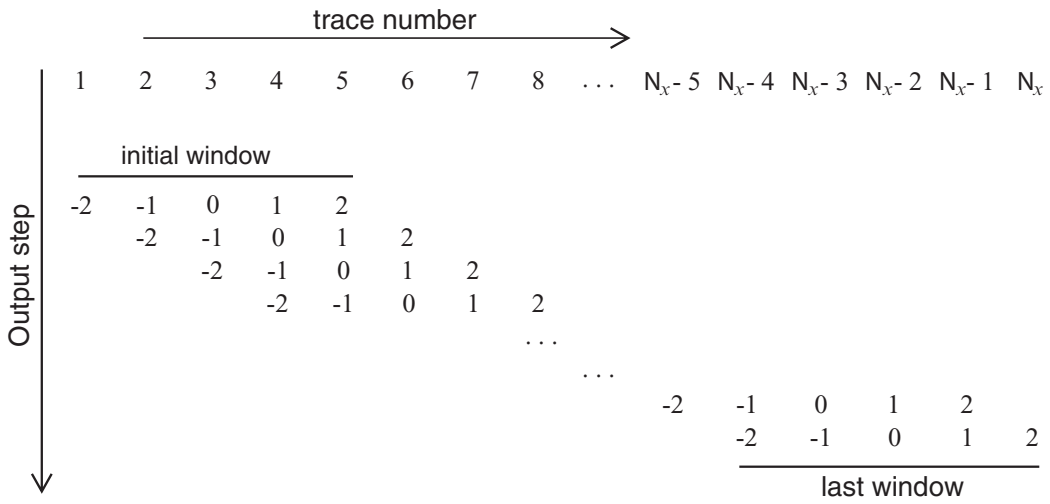

Figure 1 Sliding window SVD filtering scheme.

the SVD operator ($i = 0$). And to reinforce the spatial coherence of the reflectors we stack the centred $2L + 1$ components ($L \leq L_x$) for $i = 0$. The filtered output at position $\{t,\ x_n\}$ is computed by using the equation

$$\tilde{d}(t, x_n) = \frac{\sum_{j=-L}^{L} \left(\sum_{k=1}^{K} \sigma_k u_k(0) v_k(j) \right)}{2L + 1}. \tag{7}$$

The procedure is started at $n = L_x + 1$ and $t = L_t + 1$. Then n and t are increased by one until $n = N_x - L_x$ and $t = N_t - L_t$, respectively. For $n \leq L_x, n \geq N_x - L_x, t \leq L_t$, and $t \geq N_t - L_t$ the filtered output is obtained using the K first SVD components given by equation (6).

As in the previous case the result is a filtered data set $\tilde{d}(t, x_n)$ of the same dimension as the input data set, and energy, which is not coherent along the local dip, was attenuated. Both the character and amplitude of the coherent events are well preserved as they are represented by the first eigenvalues that correspond to the largest energy. The summation in equation (7) corresponds to a local slant stack using SVD. By including all the eigenimages, it degenerates to a local dip filter. The procedure should be used with care in order to preserve the local amplitude. If the spatial summation window length ($2L + 1$) is too large, there will be smearing. And, in all cases, only the dominant events will be enhanced. This may result in a degradation of the data quality if there are crossing events.

DATA RESULTS

The proposed method of SVD filtering was tested on a land seismic line. It contains 576 shots recorded at a 4 ms sampling interval. There are 96 channels per shot in a split-spread geometry with offsets from −1050 m to −100 m and 100 m to 3850 m, and 50 m between the geophones. The distance between the shots is 50 m, giving a low CMP coverage of 48 fold.

First a standard processing sequence was applied: geometry, edit, preliminary spherical divergence correction, standard velocity analysis and NMO correction. Due to the limited CMP coverage, the data were then resorted into shot gathers before the SVD filtering was applied.

Figure 2 shows results of the SVD filtering applied to a shot gather after NMO-correction. The original data are shown in Fig. 2(a). We used a sliding window of 3 traces and only the central traces of the eigenimages (k = 1, 2, 3) are shown in Fig. 2(b–d), respectively. Figure 2(b) was obtained using the first most significant eigenvalue. We note that the horizontal events, which are associated with the reflections of interest, are well preserved. Figure 2(c) and 2(d), show the ground-roll and the remaining non-horizontal events.

After SVD filtering in the common shot domain, the data were reorganized in common-offset panels and the local dip was estimated. A 5 × 5 matrix operator was used to compute the local derivatives and local dips as described in the Appendix. Figure 3(a) shows the estimated horizontal derivative and Fig. 3(b) shows the vertical derivative. The estimated local dip is shown in Fig. 3(c).

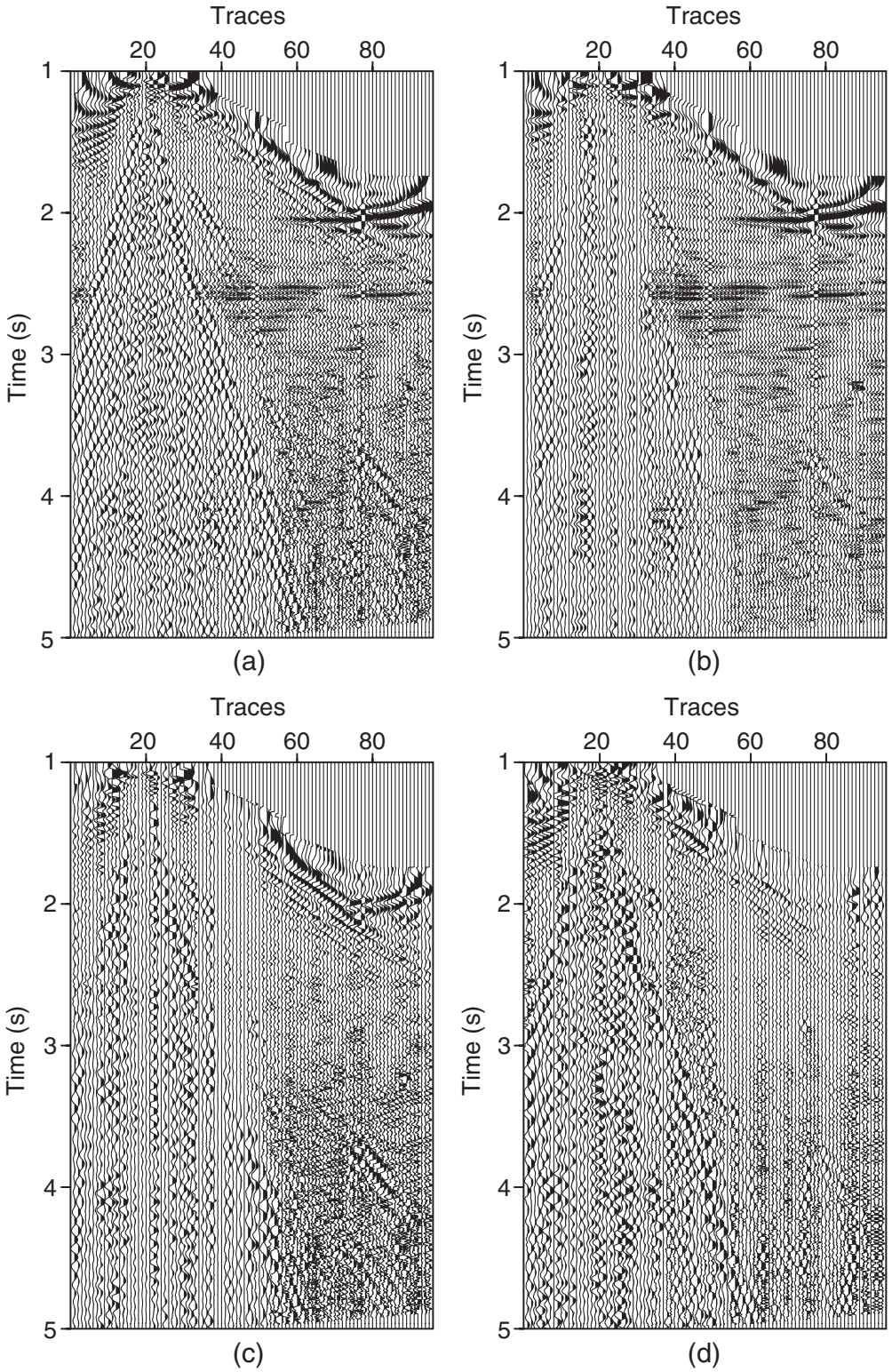

Figure 2 Comparison of SVD filtering of a shot gather corrected for NMO by using a spatial window of 3 traces. Input data in (a) and SVD with the first, second and third eigenimages in (b), (c) and (d), respectively.

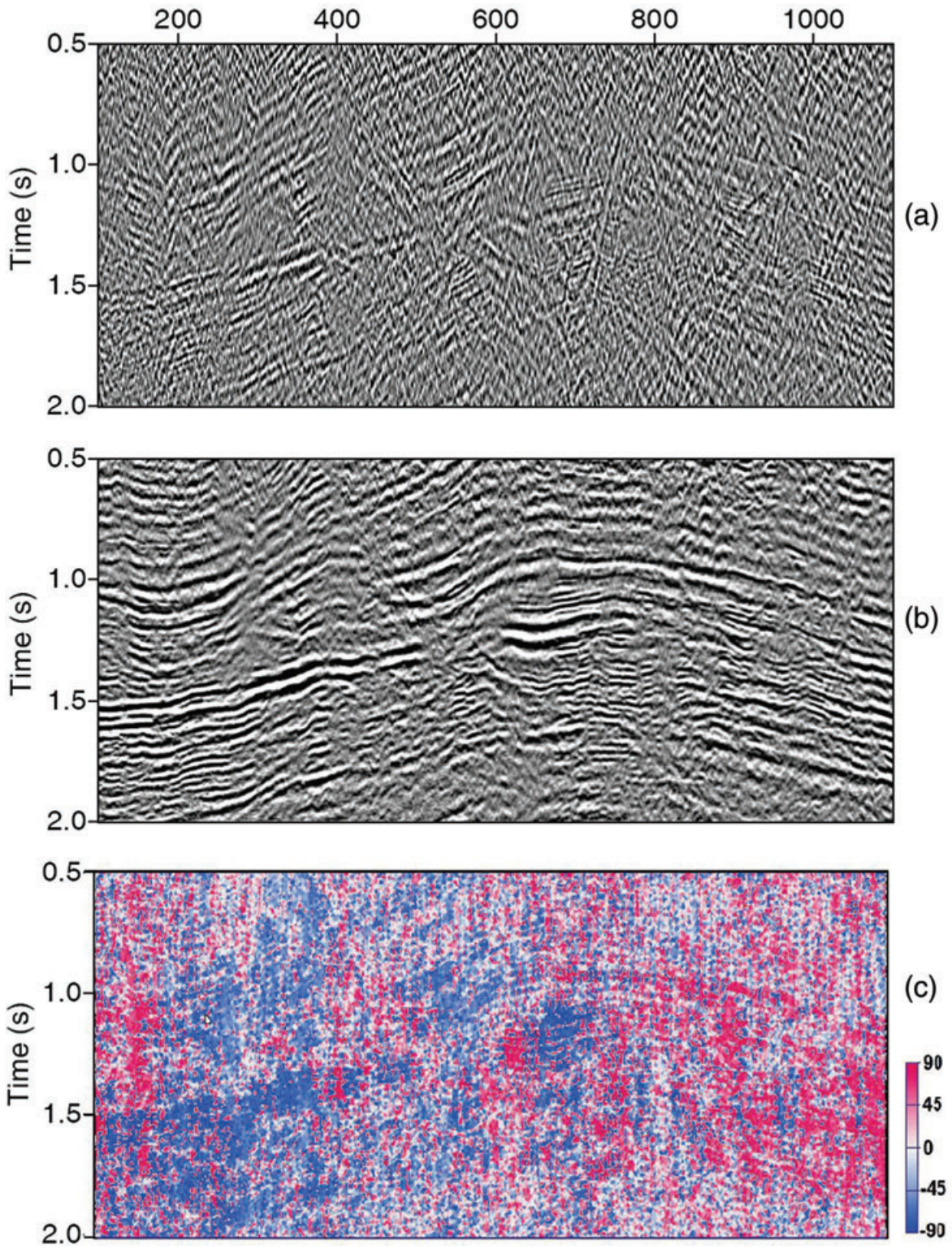

Figure 3 The estimated horizontal derivative of data (a) and the vertical derivative (b). The estimated local dip is shown in (c).

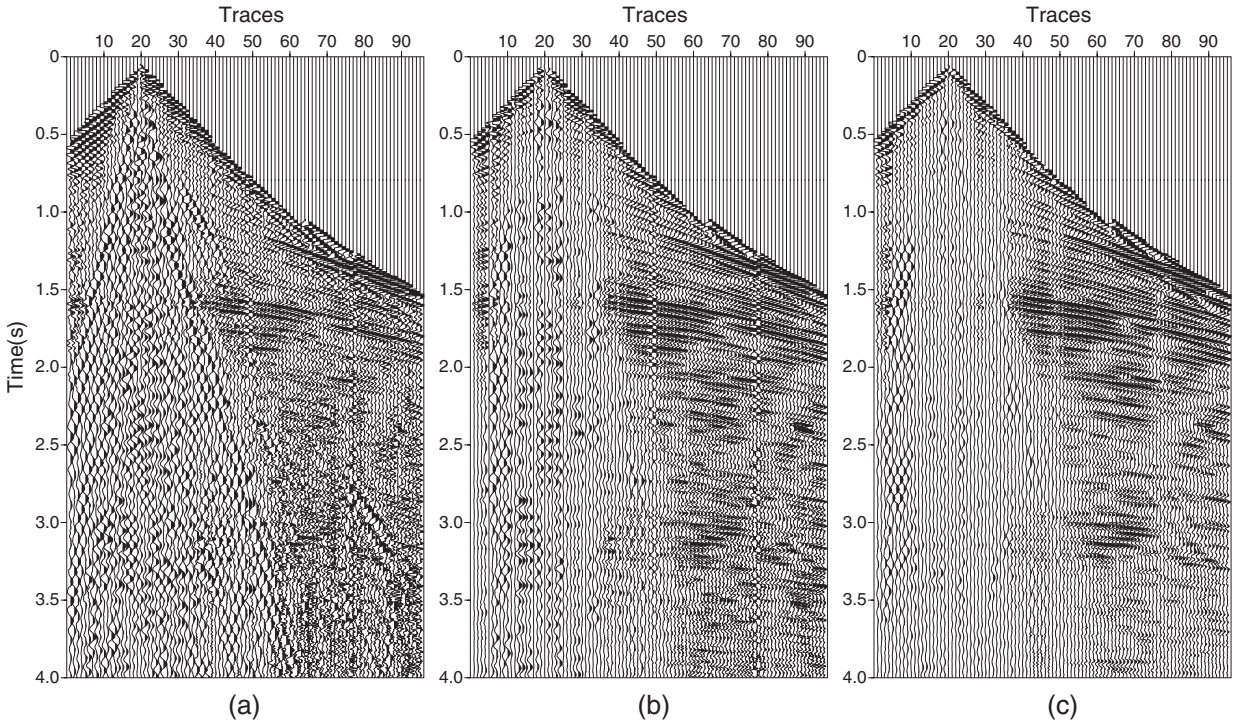

Figure 4 Original shot gather (a), the same after one pass of SVD filtering (b), and after a second pass of SVD filtering (c).

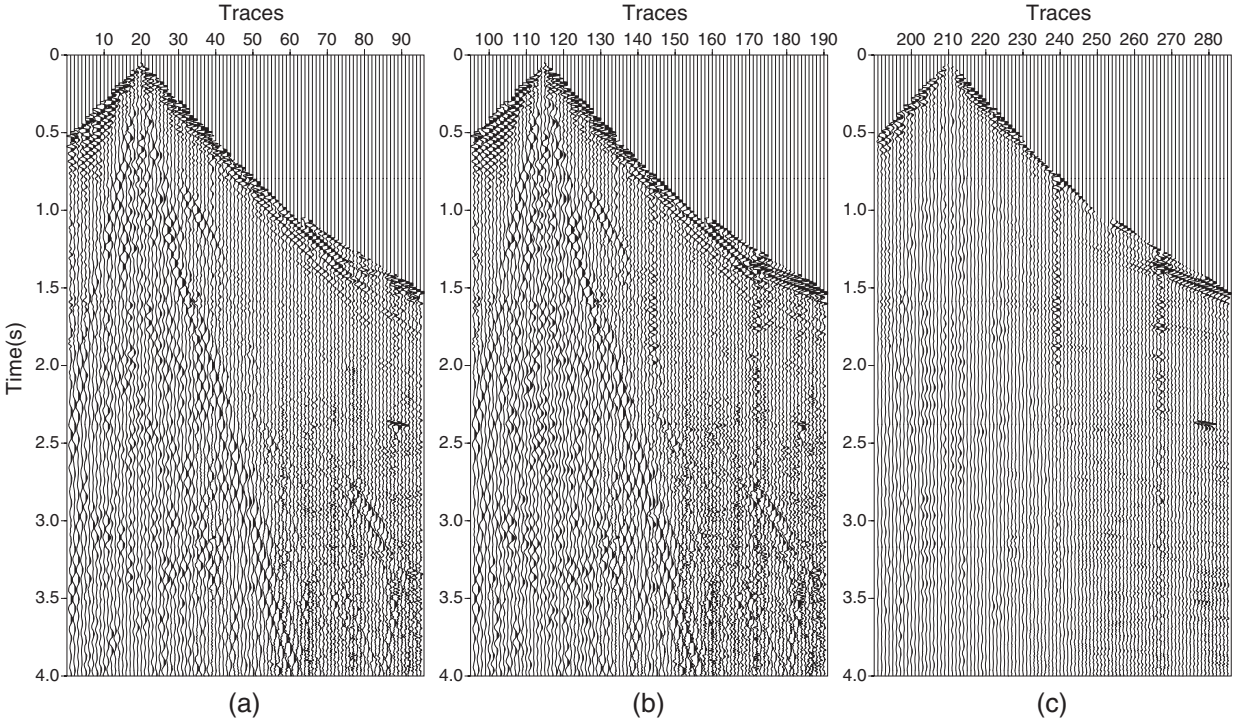

Figure 5 Noise removed by SVD filtering. First pass of SVD filtering (a), First and second pass of SVD filtering (b), and only the second pass of SVD filtering (c).

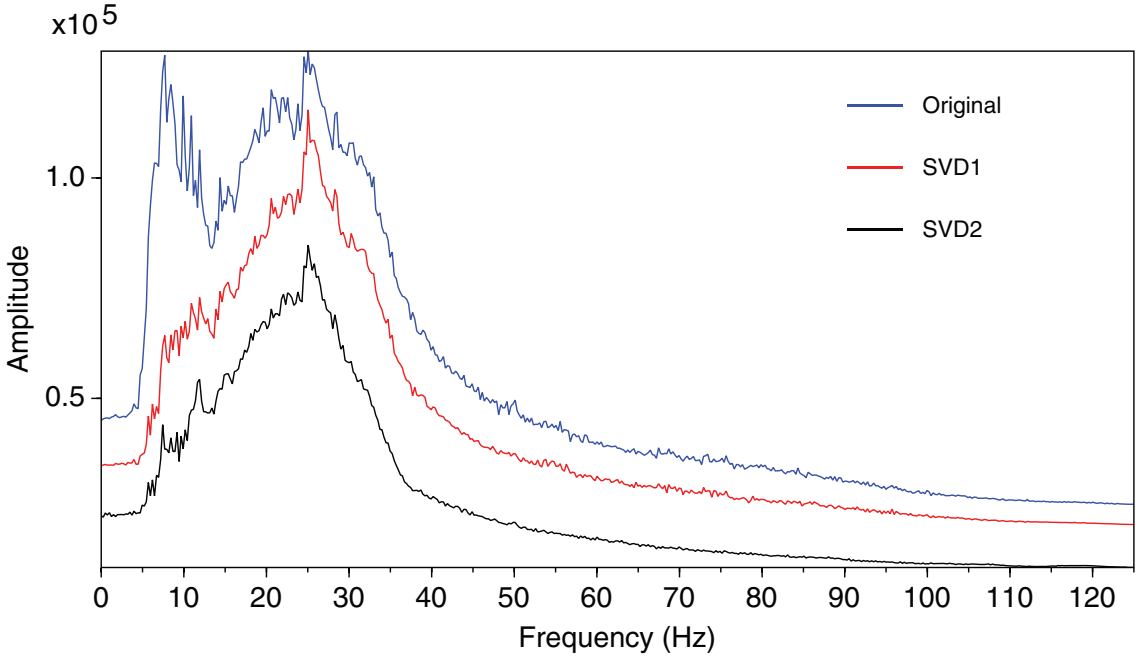

Figure 6 Average amplitude spectrum of the shot gathers in Fig. 4. Original corresponds to Fig. 4(a), SVD1 to Fig. 4(b) and SVD2 to Fig. 4(c).

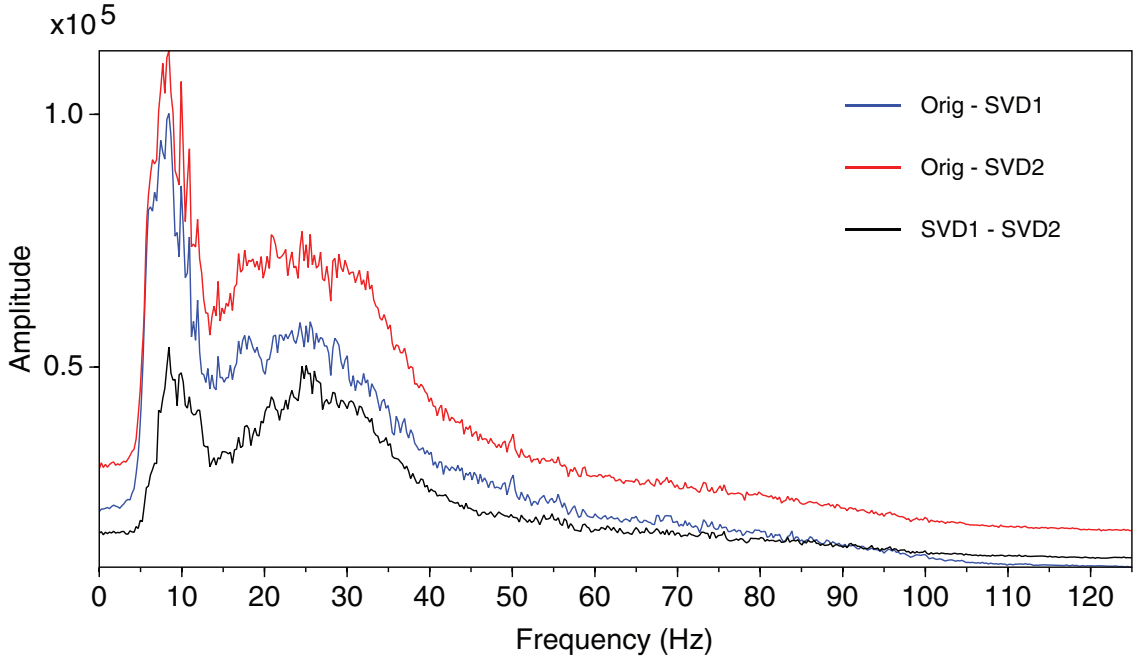

Figure 7 Average amplitude spectrum of the noise gathers in Fig. 5. Orig-SVD1 corresponds to Fig. 5(a), Orig-SVD2 to Fig. 5(b) and SVD1-SVD2 to Fig. 5(c).

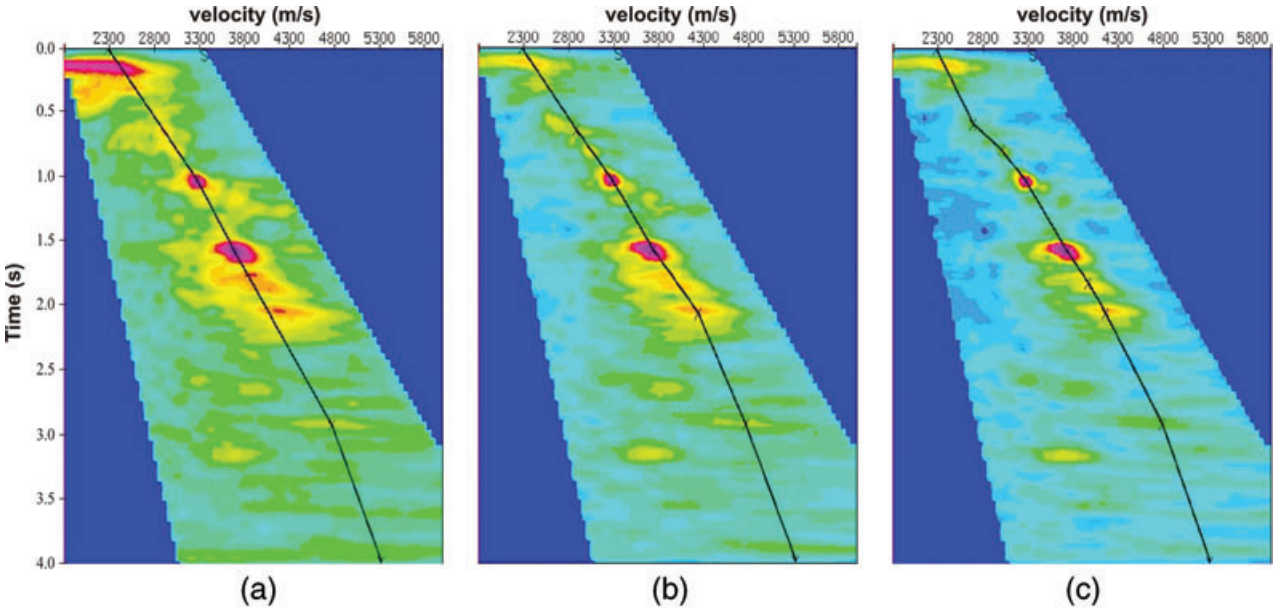

Figure 8 Velocity analysis plots corresponding to the three gathers in Fig. 4 with matching (a), (b), and (c).

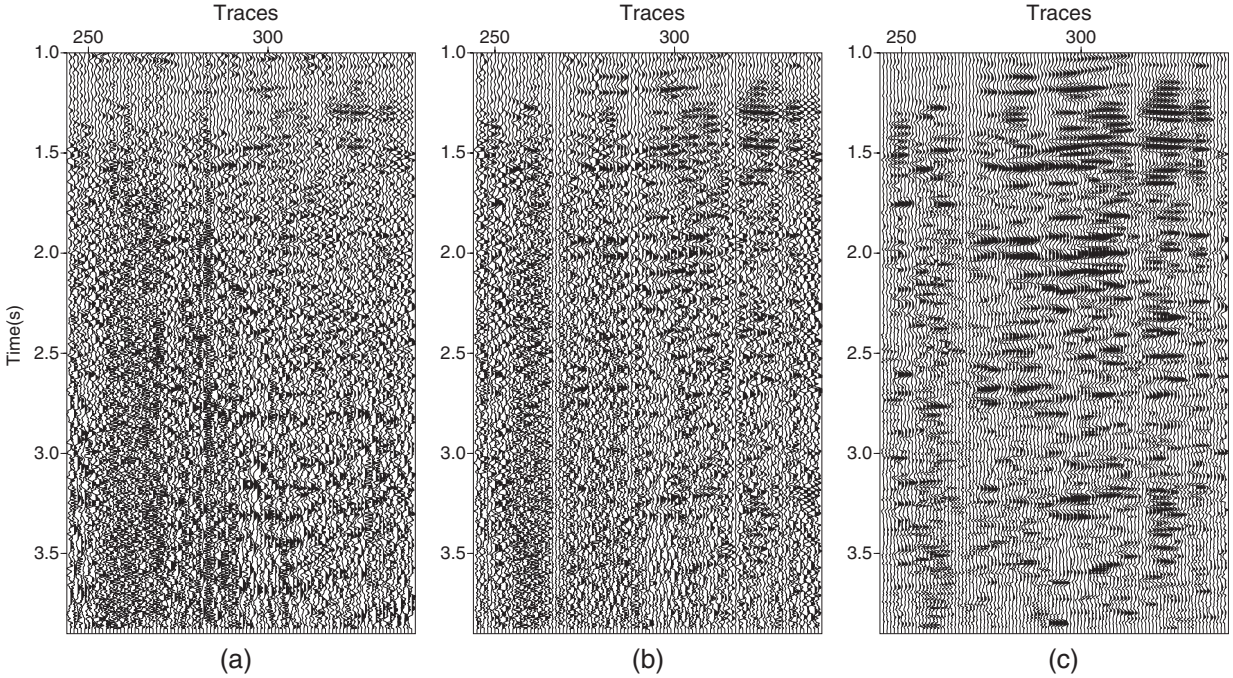

Figure 9 Part of a common-offset panel at 2050 m (a), the same after SVD filtering in the shot domain (b), and, finally, after addition filtering in the common-offset domain (c).

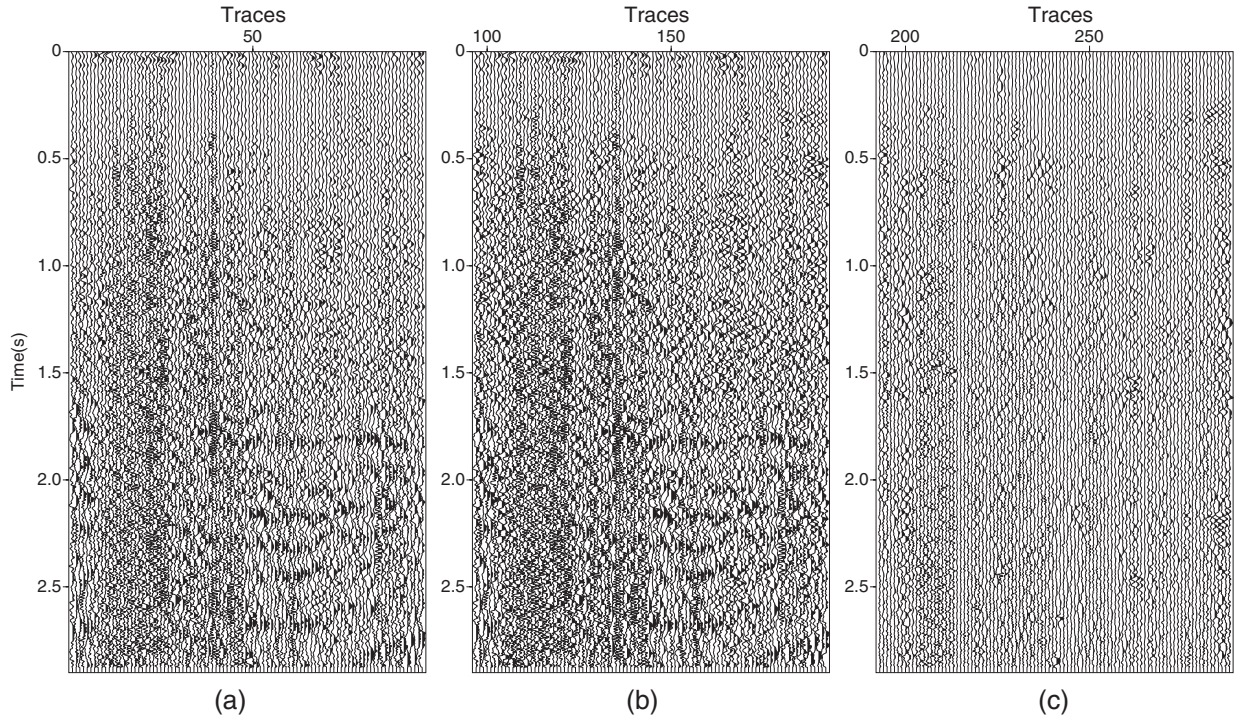

Figure 10 Removed noise in common offset panels. After one pass of SVD filtering (a), after two passes of SVD filtering (b), and noise removed in the second pass of SVD filtering (c).

Figure 4 shows the effect of SVD filtering of a common shot gather (in Fig. 4a). The result after SVD filtering of common shot gathers with a 5-trace sliding window is shown in Fig. 4(b). A 5×5 sample window was used in dip-adaptive SVD filtering in common-offset panels. The resulting common-shot gather is shown in Fig. 4(c) Figure 5 shows the removed noise. In Fig. 5(a) is the noise removed by the first pass of SVD filtering and in Fig. 5(b) is the noise removed by the two passes of SVD filtering. The noise removed by the second pass of SVD filtering (the difference between Fig. 4b and 4c) is shown in Fig. 5(c).

The average amplitude spectrum of the traces in the gathers in Fig. 4 are shown in Fig. 6 where original (blue) corresponds to the input data in Fig. 4(a), SVD1 (red) to the data after the pass of SVD filtering in Fig. 4(b) and SVD2 (black) to the data after a second pass of SVD filtering in Fig. 4(c). The average amplitude spectrum of the traces in the noise gathers in Fig. 5 are shown in Fig. 7. Orig-SVD1 (blue) corresponds to the noise removed after one pass of SVD filtering (Fig. 5a), Orig-SVD2 (red) corresponds to the noise removed after two passes of SVD filtering (Fig. 5b) and SVD1-SVD2 (black) corresponds to the noise removed in the last pass of SVD filtering (Fig. 5c).

Figure 8 shows the velocity analysis of the three gathers in Fig. 4. The focusing effect of noise removal is evident.

Figure 9(a) shows part of a common-offset gather at 2050 m. Figure 9(a) shows the same after SVD filtering in the common-shot domain. Figure 9(c) shows the result after additional SVD filtering in the common-offset domain. The noise removed in the different steps is shown in Fig. 10. Figure 10(a) shows the noise removed by SVD filtering in the shot domain and Fig. 10(b) shows the noise removed by also including SVD filtering in the offset domain. Figure 10(c) shows the noise removed in the last step. From Fig. 9 and 10 it is seen that the first step of SVD filtering removes most of the low-frequent noise while the second step removes mostly random noise. The last effect is seen by comparing Fig. 9(b) and 9(c).

The stacked section obtained from the original data is shown in Fig. 11(a). This should be compared with the stacked sections obtained by SVD filtering on shot gathers (Fig. 11b.) and followed by SVD filtering on common offset panels (Fig. 11c). Both results show an enhancement of the reflections and significant noise attenuation. However, the result obtained by a second pass of SVD filtering shows an additional improvement.

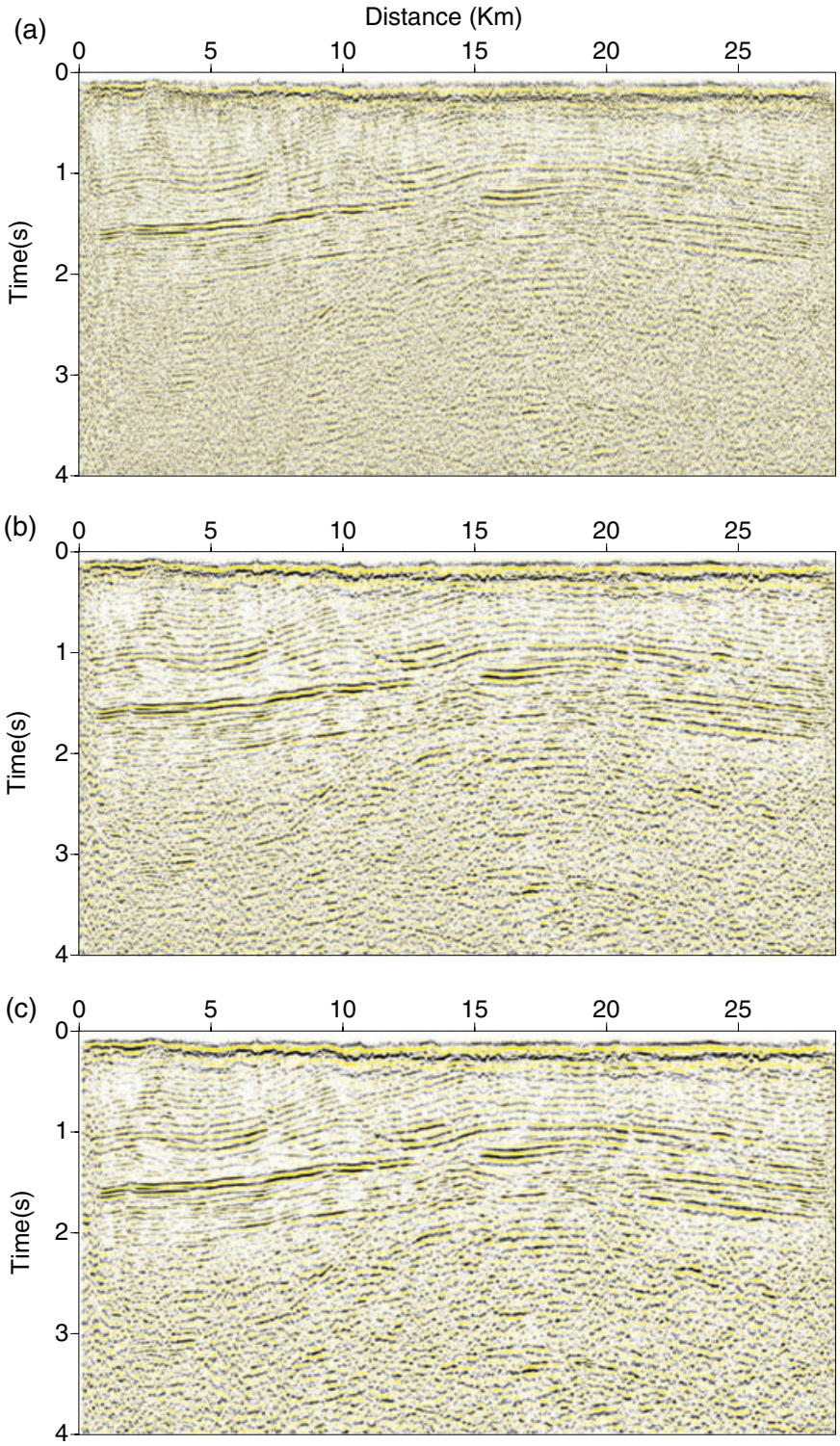

Figure 11 Stacked sections. Original data (a), SVD filtered data in the shot-gather domain (b) and SVD filtered data in the shot-gather domain followed by the common-offset domain (c).

CONCLUSION

We have developed a new and efficient SVD filtering procedure that enhances reflections and dipping events on seismic sections. Firstly, SVD filtering is applied to common-shot gathers or CMP gathers that were corrected for NMO. A sliding SVD filter preserves reflections that are horizontally aligned. Secondly, SVD filtering is applied in local windows on common-offset sections. In each window, the dominant local dip is estimated and a linear moveout correction is applied before SVD filtering. The SVD filter process preserves the character and frequency content of the reflections and attenuates all other types of events. The method was successfully applied to ground-roll attenuation on a land seismic data set. In particular, ground-roll was virtually absent from the filtered pre-stack gathers.

ACKNOWLEDGEMENTS

The authors wish to express their gratitude to INCT-GP/CNPq/MCT and PETROBRAS, FINEP, FAPESB Brazil for financial support. We also thank PARADIGM and LANDMARK for the licenses granted to CPGG-UFBA. Bjorn Ursin has received financial support from the VISTA project and from the Norwegian Research Council through the ROSE project.

REFERENCES

Bekara M. and van der Baan M. 2007. Local singular value decomposition for signal enhancement of seismic data. *Geophysics* **72**, 59–65.

Chiu S.K. and Howell J.E. 2008. Attenuation of coherent noise using localized-adaptive eigenimage filter. *SEG, Expanded Abstracts* **27**, 2541–2545.

Freire S.L.M. and Ulrych T. 1988. Application of singular value decomposition to vertical seismic profiling. *Geophysics* **53**, 778–785.

Golub G.H. and van Loan C.F. 1996. Matrix Computations. Johns Hopkins University Press.

Liu X. 1999. Ground roll suppression using the Karhunen-Loeve transform. *Geophysics* **64**, 564–566.

Melo P., Porsani M. and Silva M. 2009. Ground-roll attenuation using a 2D time-derivative filter. *Geophysical Prospecting* **57**, 343–353.

Porsani M., Silva M., Melo P. and Ursin B. 2009. Ground-roll attenuation based on SVD filtering. *SEG Expanded Abstracts* **28**, 3381–3385.

Porsani M., Silva M., Melo P. and Ursin B. 2010a. SVD filtering applied to ground-roll attenuation. *Journal of Geophysics and Engineering* **7**, 284–289.

Porsani M., Silva M., Melo P. and Ursin B. 2010b. An adaptive local-slope SVD filtering approach to enhance events on seismic sections. *SEG Expanded Abstracts* **29**, 3717–3722.

Schleicher J., Costa J.C., Santos L.T., Novais A. and Tygel M. 2009. On the estimation of local slopes. *Geophysics* **74**, 25–33.

Tyapkin Y.K., Marmalyevskyy N.Y. and Gornyak V. 2003. Source-generated noise attenuation using the singular value decomposition. *SEG Expanded Abstract* **22**, 2044–2047.

Van Huffel S. and Vandewalle J. 1991. *The total least squares problems: Computational aspects and analysis*. SIAM, Philadelphia.

APPENDIX A

Local dip estimation

Assuming that the reflected seismic wave has locally linear moveout, $d(t, x) = s(t - px)$, the local dip estimation may be computed as the ratio between the derivatives of the seismic data with respect to t and x,

$$p = -\frac{\partial d}{\partial x} \Big/ \frac{\partial d}{\partial t}. \tag{A1}$$

There are several methods to estimate the derivatives regarding x and t available in the literature. In the numerical examples we have used the approach proposed by Melo et al. (2009). From the input data matrix we obtain two other matrices, corresponding to the derivatives with respect to x and t, respectively.

At each output point (t, x_n) we consider the derivatives in a rectangle $(t + i, x_{n+m})$, $L_t \leq i \leq L_t$, $-L_x \leq m \leq L_x$, and collect them into the vectors $\boldsymbol{d}_t$ and $\boldsymbol{d}_x$.

However, since we have errors on both variables, the solution may be obtained through the total least squares method (Van Huffel and Vandewalle 1991). In this case the residual is defined as the shortest distance between the data point and the fitted straight line,

$$\boldsymbol{d}_x + p\boldsymbol{d}_t = 0. \tag{A2}$$

The local dip is obtained by solving the following eigenvalue problem:

$$\begin{bmatrix} \boldsymbol{d}_x^T \boldsymbol{d}_x & \boldsymbol{d}_x^T \boldsymbol{d}_t \\ \boldsymbol{d}_t^T \boldsymbol{d}_x & \boldsymbol{d}_t^T \boldsymbol{d}_t \end{bmatrix} \begin{bmatrix} 1 \\ p_j \end{bmatrix} = \sigma_j^2 \begin{bmatrix} 1 \\ p_j \end{bmatrix}, \quad j = 1, 2. \tag{A3}$$

The local dip p is the value p_j corresponding to the smallest eigenvalue σ_j^2. Other approaches for local dip estimation may be found in Schleicher et al. (2009).